Int j simul model 24 (2025) 4, 623-634
Original scientific paper

COLLAPSED PARTICLES VELOCITY ANALYSIS IN DRILL HOLE BASED ON CFD–DEM

Xu, B. L.[*,**]; Zhang, X. D.[***,#]; Ye, S. X.[****] & Guo, S. S.[**]

[*] Key Laboratory of Xinjiang Coal Resources Green Mining, Ministry of Education, Xinjiang Institute of Engineering, Urumqi 830023, China

[**] School of Safety Science and Engineering, Xinjiang Institute of Engineering, Urumqi 830023, China

[***] College of Mechanical and Electronic Engineering, Shandong University of Science and Technology, Qingdao 266590, China

[****] Xi'an Research Institute, China Coal Technology & Engineering Group, Xi'an 710077, China

E-Mail: zhangxd061@foxmail.com ([#] Corresponding author)

Abstract

To optimize the key parameters of pipe-following drilling with spiral casing in underground spaces, the analysis model including different particle sizes, borehole water flow velocities, and casing rotational speeds is established using the CFD–DEM method. FLUENT and EDEM software are used to analyse the relationship between the axial migration velocity of particles and the velocity of water flow and the rotational speed of spiral casing. Results show that the axial conveying velocity of particles has a linear relationship with the velocity of water flow, and it exhibits a power function relationship with the rotational speed of casing. Under the coupling effect of water flow and casing rotation, increasing the velocity of water flow has no obvious effect on improving the axial migration velocity of particles when the rotational speed is low. When the rotational speed exceeds 120 rpm, increasing the water velocity can obviously improve the axial migration velocity of particles with the increase in rotational speed. This research provides a reference for the optimal drilling process and selection of key parameters for pipe-following drilling with spiral casing.

(Received in August 2025, accepted in November 2025. This paper was with the authors 1 month for 1 revision.)

Key Words: Numerical Simulation, Spiral Casing, Water Flow Velocity, Rotational Speed, Axis Conveying Velocity

1. INTRODUCTION

Advanced drilling borehole plays an important role in exploitation disasters before tunnel (roadway) excavation and exploration of underground resources and energy [1]. However, under the multiple coupling of geological factors such as stratigraphic joints, bedding, and original crushing with in situ stress and flushing media [2-5], a risk of collapse and instability of boreholes exists, which results in the depth of advanced boreholes not reaching the design position. The pipe-following drilling technology can realize the immediate follow-up of the casing while drilling, which is an effective method to deal with complex strata, protect the borehole wall, and extend the drilling depth [6].

Pipe-following drilling technology was initially used in the field of vertical drilling on the ground. The casing is in a non-rotating state, and the flowback of drilling cuttings depends on the upward carrying capacity of the drilling fluid enhanced by a treatment agent. However, for the near-horizontal drilling conditions in underground spaces, the capability of the flushing fluid to carry drilling cuttings is significantly weakened due to the use of air and water as the flushing medium [7]. The casing in a non-rotating state is also prone to sticking accidents due to deposited drill cuttings. Relevant research results show that the cutting flowback effect of horizontal holes can be significantly improved when the string is rotated [8]. Therefore, relevant research institutions have developed an air drilling technology using a double-powered rotary head and double-tube system for broken soft coal seams in coal mines [9, 10]. To simplify the requirements of the equipment and improve its universality, the author proposes a hole bottom-driven pipe drilling technology for broken strata in underground spaces; the rotation of the casing is realized through the hole bottom-driven device without changing the existing construction equipment [11]. This technology combined with spiral casing is used to solve the problem of hole protection while drilling in broken formation. The aim is to improve the rate and depth of hole formation in broken strata. When drilling in broken and easy-to-collapse strata, achieving an efficient flowback of collapsed blocks is important to improve construction efficiency and reduce drilling accidents.

2. STATE OF THE ART

Theoretical calculation, numerical simulation, and laboratory test are the three main methods to study drilling slag migration in holes [12]. In the absence of rotational disturbance caused by special-shaped drilling tools, the migration of drilling slag in the hole mainly depends on the carrying effect of the drilling fluid. Cho et al. [13], Kelessidis and Bandelis [14], Hou et al. [15] have divided the motion state of drilling slag in horizontal or inclined drilling holes into eight types: uniform suspension, non-uniform suspension, formation of slip layer, forward movement of slip layer, sand dune movement, and Boycott movement. Zhang et al. [16] used the basic principle of fluid mechanics to derive the mechanical formula of the hydraulic loss along the flushing fluid circulation process during the drilling of the anchor hole and the upward return of the drilling slag in the flushing fluid under the solid–liquid coupling effect. Based on the theory of powder mechanics, Wang et al. [17] established a mechanical model of the blockage section of gas extraction boreholes, deduced the relationship equation between the dredging pressure and the length of the blockage section, and emphatically analysed the influence of lateral pressure coefficient and borehole dip angle on borehole blockage. Pan et al. [18] analysed the stability of nitrogen foam, the fluidity of foam in drill pipe, drill bit, and annular space, the suspension performance of pulverized coal in foam, the pressure loss of foam slag discharge in annular space, and the force of foam upward slag discharge by power law multiphase flow theory. To reveal the law of drilling slag migration in the hole from the micro level and provide theoretical support for the optimization of drill pipe and construction parameters, many scholars have used numerical simulation methods for analysis. Wang et al. [19] regarded the mixture of water and slag as a non-Newtonian body with a certain density. They used FLUENT to analyse the influence of the width, depth, and pitch of the spiral groove of the grooved drill pipe on the slag discharge effect. Liu et al. [20] used the standard three-dimensional turbulence model in the solid–liquid two-phase flow theory of the Euler model to perform a three-dimensional dynamic analysis of the drilling slag migration process in the small-aperture floor anchoring hole under different conditions. They obtained the slag removal effect under different combinations of influencing factors. Fu et al. [21] used a multiphase flow numerical simulation method to study the migration characteristics of drilling slag and the influencing factors of small-diameter anchor holes in the floor strata. Mao et al. [22] studied the effects of airflow velocity, cutting concentration, drilling speed, particle diameter, and inclination angle on cutting transport in air reverse circulation drilling in tunnel construction using a multiphase flow numerical simulation method. Jiang et al. [23] used a numerical simulation method combining continuous and discrete phases to study the influence of the outlet diameter, inlet diameter, and outlet length of the shaft boring machine on the slag discharge performance. To overcome the difficulty of directly reflecting the movement process and interaction of particles in the numerical simulation of multiphase flow, a numerical simulation method based on CFD–DEM is widely used to study drilling slag migration in holes. DEM has been widely used in the field of particle transportation [24]. Combined with fluid simulation software, it can effectively simulate the interaction and motion characteristics of drilling cuttings during drilling. Yu et al. [25] used a CFD–DEM numerical simulation method to study the influence of cutting bed cleaner on drilling slag migration. Akhshik et al. [26] presented a coupled CFD and DEM approach to simulate cutting transport considering the dynamic collision process. In addition, some scholars have used DEM alone to simulate the transport behaviour of particle flow [27, 28].

In the abovementioned CFD–DEM coupling simulation study, the drilling slag is equivalent to a sphere of the same diameter, and the irregularity of the drilling cuttings in the actual drilling process is ignored. In particular, the migration law of large particles of drilling slag caused by the collapse of the hole wall has not been reported. In addition, research on the coupling effect of spiral blade rotary conveying and flushing medium has not been systematically conducted.

The rest of the paper is organized as follows. In the third part, the analysis model including different particle sizes, borehole water flow velocities, and casing rotational speeds based on the CFD–DEM method, material parameters, and simulation parameter settings are introduced in detail. In the fourth part, the single and coupling relationships between the axial conveying velocity and water flow velocity and casing rotational speed are analysed. The conclusions are provided in the fifth part.

3. METHODOLOGY

3.1 Geometric model of coupled particle migration

In the discrete element simulation, the simulated borehole and spiral casing are set as the wall, that is, the rigid body material. The structural size is shown in Fig. 1 a, and the detailed description is given in Table I. The long drilling length in the actual drilling construction in the underground space causes difficulty in establishing a full-scale numerical simulation model. The 1 m drilling length is used to improve the simulation efficiency, as determined in the discrete element simulation. In addition, considering that the casing is in contact with the bottom of the hole wall under the action of gravity during the actual horizontal drilling process, the spiral casing and the borehole are eccentrically set in the simulation, and the eccentric distance is 6 mm. Using the fluid simulation software FLUENT, a liquid environment is provided for the transportation of cutting particles in the borehole. The fluid calculation model is built in FLUENT. The steps of established model are discussed as follows:

(1) The fluid domain is extracted according to the geometry of the inner wall of the borehole and the spiral casing. The fluid domain adopts a tetrahedral mesh. Given that the minimum particle size is 15 mm, the mesh size of the fluid domain is 3 mm.

(2) The dynamic mesh is compiled according to the structural parameters and rotational speed of the spiral casing. In this way, the fluid domain in FLUENT is consistent with the wall motion in the discrete element simulation.

(3) The velocity inlet is set at one end of the particle factory in the corresponding discrete element, the gas–liquid two-phase flow is set in the fluid domain, and the steady-state analysis is started. When the borehole is completely liquid phase, the steady-state analysis result is used as the initial result of the transient analysis of the solid–liquid two-phase coupling.

(4) By compiling the coupling interface file, the discrete element file is connected with FLUENT to conduct two-way coupling simulation.

At the same time, a particle factory is set at the starting position of transportation, and the particles fall freely under the action of gravity to simulate the effect of borehole collapse in broken strata. The proportion of different sizes of rock debris particles in the particle factory is set as shown in Fig. 1 b. The quantity and mass ratios of different particles are shown in Figs. 2 a and 2 b, respectively. The specific modelling process of the particle factory is as follows:

(1) Drilling cuttings are collected from the construction site.

(2) The cuttings are classified according to size, which is divided into four levels of < 15 mm, 15–25 mm, 25–35 mm, and > 35 mm.

(3) The non-contact laser three-dimensional scanner is used to scan and model the rock debris particles with a diameter of > 15 mm, and the three-dimensional model of high-precision point cloud in STL format is obtained.

(4) The STL format model of rock debris particles obtained by scanning is used as a template to fill with hard sphere particles to construct a discrete element particle model of rock debris with a complex morphology.

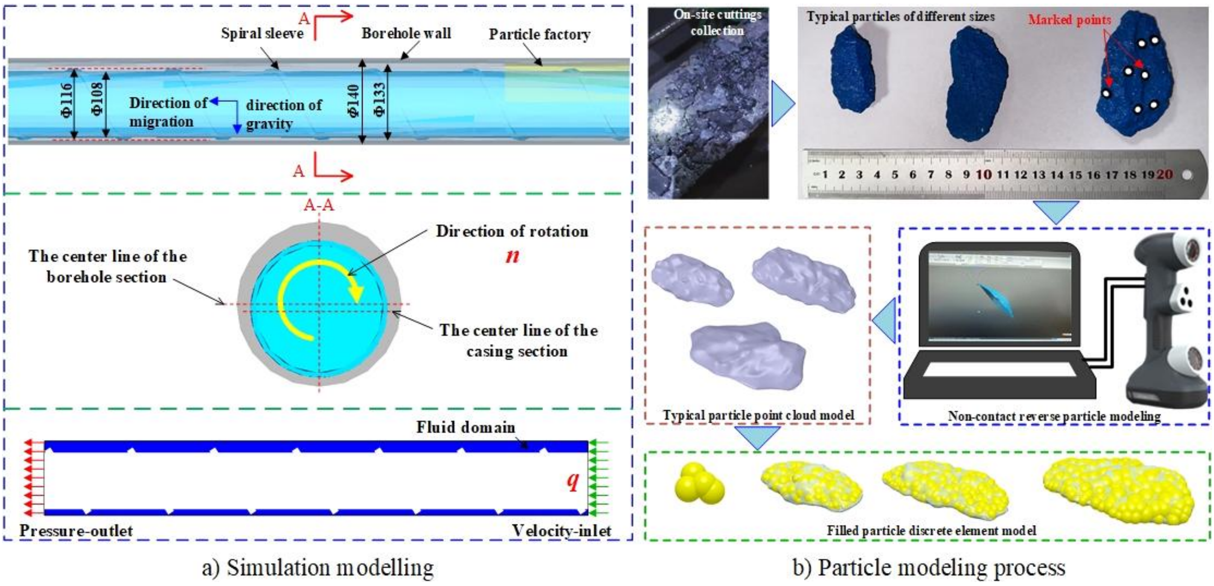

Figure 1: Modelling process of the geometric model.

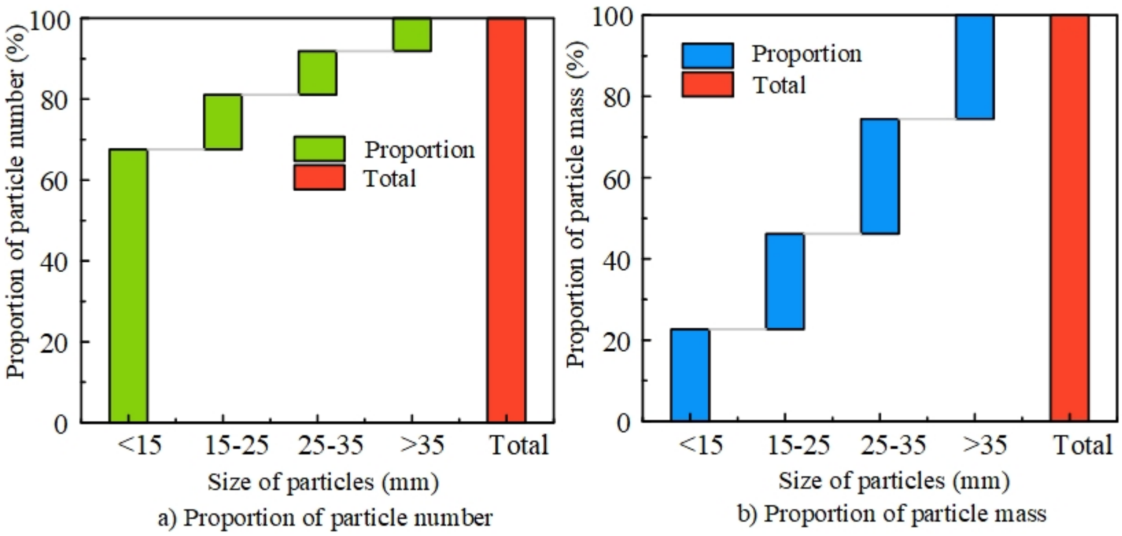

Figure 2: Proportion of particles with different particle sizes.

3.2 Material properties

The material properties of the particles and the contact parameters between the particles and the wall in the discrete element simulation have an important influence on the motion behaviour of the particles. Based on the existing research on the calibration results of the discrete element particle material, the particle and wall material parameters in the simulation are given in Table I.

Table I: Main parameters of the material.

	Poisson's ratio	**Young's modulus** (GPa)	**Density** (kg/m^3)
Particle	0.26	25.4	2600
Wall	0.28	204	7850
	Elastic restitution coefficient	**Rolling friction coefficient**	**Sliding friction coefficient**
Particle-particle	0.20	0.15	0.80
Wall-particle	0.24	0.10	0.60

3.3 Simulation scheme

As shown in Fig. 1 a, the water flow velocity is q, and the rotational speed of casing is n. The particles move outside the hole under the coupling effect of the drag force of the fluid and the spiral conveying of the spiral casing. The values of q and n are shown in Table II.

Table II: Simulation variables.

$\boldsymbol{q}$ (m/s)	$\boldsymbol{n}$ (rpm)
0.71, 0.89, 1.07, 1.24, 1.45	60, 120, 150, 180

4. RESULTS AND DISCUSSION

4.1 Comparison of traditional casing and spiral casing

Fig. 3 a shows that the particles are generated from the particle factory and settle to the bottom of the borehole under the action of gravity. Some small debris particles are suspended in the borehole under the action of water flow because of their small volume and mass, and they move axially with the action of water flow. The figure also shows that the axial velocity is close to the flow velocity. The large debris particles are concentrated at the bottom of the hole, and the axial velocity is small. From t = 0.6 s to t = 3.6 s, the axial displacement is not obvious. Effectively discharging large-size rock slag is difficult when using ordinary casing. Fig. 3 b shows that, under the action of spiral casing, the large debris particle group settles at the bottom of the borehole and the axial velocity is small when t = 0.6 s. When t = 1.6 s, the spiral casing rotates one circle, and the spiral stirs and settles the large debris particle group at the bottom of the borehole. At this time, the axial velocity of the particles increases significantly and moves axially under the driving effect of the water flow. From the stages of t = 1.6–2.6 s and t = 2.6–3.6 s, the spiral casing periodically stirs the large particle group, avoids its deposition at the bottom of the hole, and increases its axial movement speed. This result can be further confirmed by the particle trajectory diagram shown in Fig. 4.

To quantitatively compare the lifting effect of the spiral and ordinary casing conditions, the comparison results of the axial conveying velocity of particles in the borehole corresponding to the two casings are given in Fig. 5 a. The figure shows that, under the two casing conditions, the axial flow velocity of the particles in the borehole increases gradually with the decrease in the particle size of the cuttings, which corresponds to the particle motion in Fig. 3. Comparison of the axial flow velocity of the particles in the spiral and ordinary casing conditions shows that the spiral casing has a significant effect on the axial movement of the particles in the auxiliary drilling, especially for the larger cutting particles. Specifically, the corresponding average axial flow velocity of particles is approximately 2.5 times that of the ordinary casing (Fig. 5 b). This result further confirms the superiority of the spiral casing for the slag removal effect of the underground horizontal drilling.

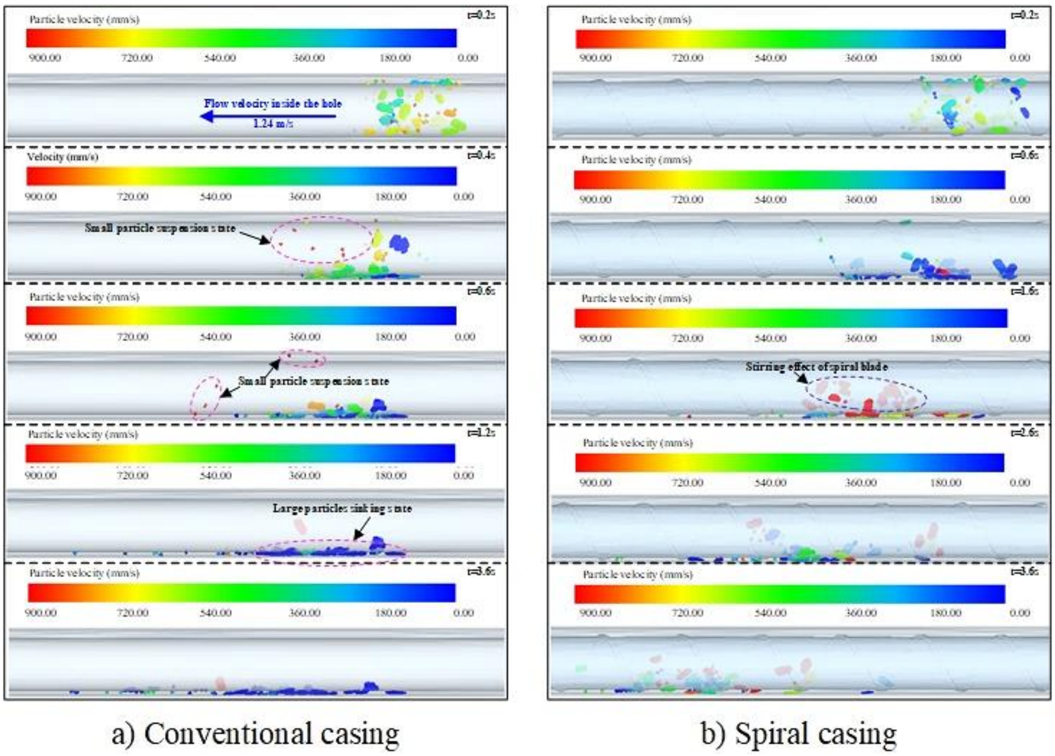

Figure 3: State of particles in the borehole at different times.

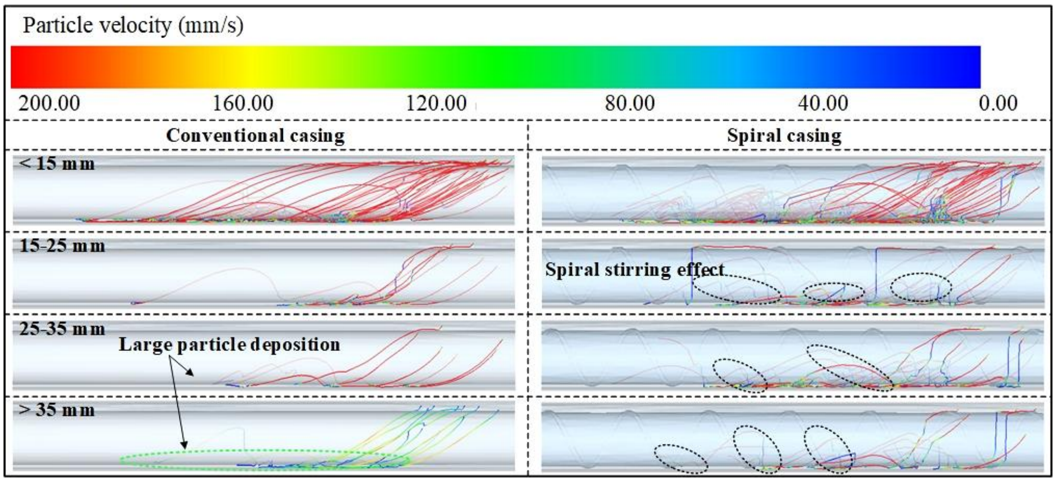

Figure 4: Migration trajectory line of particles.

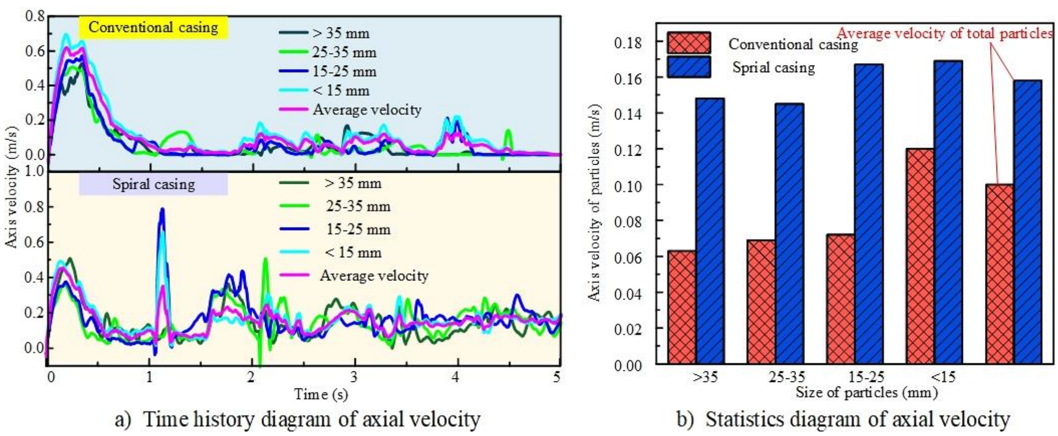

Figure 5: Axial conveying velocity of particles.

4.2 Effect of rotational speed

According to the range of casing speed in Table II, the law of particle velocity changing with casing speed under different water flow velocities in the hole is obtained by simulation. The time domain curves for the axial migration velocity of particles corresponding to four different speeds under a water flow velocity of 1.45 m/s are given in Fig. 6 a.

The geometric length of the borehole established in the simulation is 1 m. Fig. 6 a shows that, when the flow velocity in the borehole is constant, the increase in the rotational speed of spiral casing raises the average velocity of the particles moving along the axial direction of the borehole. As a result, the time of the particles in the borehole in the simulation domain gradually decreases. When the rotational speed of spiral casing increases from 60 rpm to 180 rpm, the time of particles in the borehole is shortened from 3.75 s to 1.2 s, which further illustrates that the rotational speed of casing has a significant effect on the axial flow of particles.

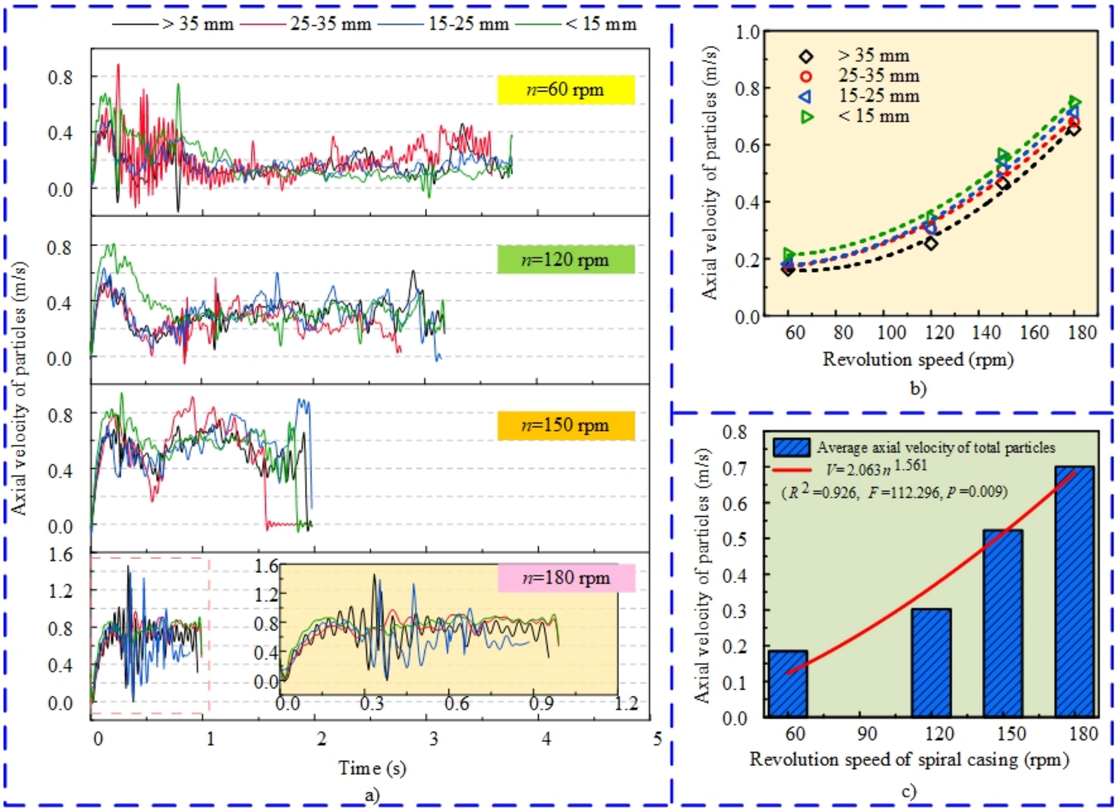

Figure 6: Axial conveying velocity of particles under different rotational speeds.

To grasp the influence of the rotational speed of spiral casing on the axial flow velocity of cutting particles, the results of the axial velocity of particles with different particle sizes changing with the rotational speed of spiral casing under a water flow velocity of 1.45 m/s are given in Figs. 6 b and 6 c. Fig. 6 b shows that the axial flow velocity of cuttings with different particle sizes increases monotonously with the rise in the rotational speed of spiral casing. The relationship between the axial velocity of particles and the rotational speed of casing is analysed using linear, power, and parabolic functions. Analysis of the parameters of each regression model shows that, for describing the relationship between the axial velocity of particles with different particle sizes and the rotational speed of spiral casing in the range of 60–180 rpm, the fitting result of the parabolic function is the best. The determination coefficient R^2 of the fitting function corresponding to the four particle sizes is greater than 0.98; the second is the power function, and the fitting function R^2 corresponding to the four particle sizes is greater than 0.90. The fitting results of the linear function are relatively poor. Although the parabolic function has the best fitting results for the axial velocity of particles and the rotational speed of casing, according to construction site experience, the slag discharge effect of the spiral casing generally increases with the rise in casing speed. Therefore, according to the fitting function parameters in Table III, when the casing speed increases from 0 rpm to 60 rpm, the axial velocity of particles decreases first and then increases, which is obviously inconsistent with the actual situation. Thus, the power function should be used to describe the relationship between the axial flow velocity of particles in the borehole and the rotational speed of casing. It should also be utilized to evaluate the slag discharge characteristics in the actual drilling construction process according to the rotational speed of casing. In addition, the axial flow velocity of all cutting particles in the borehole is averaged, and the average axial flow velocity of the particles corresponding to different spiral casing speeds is obtained, as shown in Fig. 6 c. At the same time, the power function fitting is also used. The fitting results show that, within the confidence interval of 99 %, a strong power function relationship exists between the average axial flow velocity of particles and the casing speed ($R^2 > 0.90$).

Table III: Fitting results of different types of functions.

Regression model	Size	Fitting equation	R^2	F	p
Linear regression	> 35 mm	$V_z = 0.004n - 0.133$	0.888	27.078	0.035
	25–35 mm	$V_z = 0.004n - 0.117$	0.931	15.871	0.058
	15–25 mm	$V_z = 0.004n - 0.133$	0.920	23.139	0.041
	< 15 mm	$V_z = 0.004n - 0.097$	0.922	23.733	0.040
Power function regression	> 35 mm	$V_z = 6.59 \cdot 10^{-5} n^{1.768}$	0.909	82.304	0.012
	25–35 mm	$V_z = 2.39 \cdot 10^{-4} n^{1.528}$	0.940	142.458	0.007
	15–25 mm	$V_z = 1.86 \cdot 10^{-4} n^{1.586}$	0.930	115.615	0.009
	< 15 mm	$V_z = 4.49 \cdot 10^{-4} n^{1.423}$	0.921	117.025	0.009
Parabolic function regression	> 35 mm	$V_z = 3.82 \cdot 10^{-5} n^2 - 0.005n + 0.318$	0.990	47.794	0.010
	25–35 mm	$V_z = 2.93 \cdot 10^{-5} n^2 - 0.003n + 0.230$	0.990	48.743	0.011
	15–25 mm	$V_z = 3.24 \cdot 10^{-5} n^2 - 0.003n + 0.250$	0.983	28.609	0.013
	< 15 mm	$V_z = 3.34 \cdot 10^{-5} n^2 - 0.003n + 0.298$	0.990	48.181	0.010

4.3 Effect of rotational speed

To clarify the single factor's influence of the flow velocity of the borehole on the slag discharge characteristics of the large particles, the time domain curves of the axial velocity of the particles under different flow velocities at 150 rpm of the spiral casing are given in Fig. 7 a. When the flow velocity in the borehole increases from 0.71 m/s to 1.45 m/s, the time for the rock slag particles to discharge from the simulation domain in the hole gradually shortens. In addition, the axial velocity of rock slag particles with smaller particle size is significantly higher than that of rock slag particles with larger particle size, which is similar to the change rule of particle axial velocity under different casing rotational speeds. To quantify the influence of borehole flow velocity on the axial flow velocity of particles with different particle sizes, the variation law of the axial and flow velocities of particles with different particle sizes is obtained.

Fig. 7 a shows that, with the increase in the flow velocity of the borehole, the slag carrying characteristics of the water flow are enhanced, and the rock slag particles of each particle size show a linearly increasing trend. The relationship between the flow and axial velocities of particles is also fitted using the linear, power, and parabolic functions (Table IV). According to the analysis of the coefficient of determination R^2, the parabolic function is the best for describing the relationship between the flow and axial velocities of particles in the range of 0.71–1.45 m/s. However, similar to the reason for the relationship between the rotational speed of spiral casing and the axial velocity of particles, field construction experience suggests that the slag carrying effect is better when the amount of water in the borehole is large. Thus, the parabolic function is used to describe the relationship between the two. However, the fitting outcome is inconsistent with the actual situation. Therefore, the fitting equation parameters of the linear and power functions are further compared. Analysis of the regression parameters of the two fitting models shows that the linear function is more effective in describing the relationship between water flow velocity and particle axial velocity. As shown in Figs. 7 b and 7 c, a strong linear relationship exists between the flow and axial velocities of particles ($R^2 > 0.90$) in the 99 % confidence interval. According to the range of casing speed in Table II, the law of particle velocity changing with casing speed under different water flow velocities in the hole is obtained by simulation.

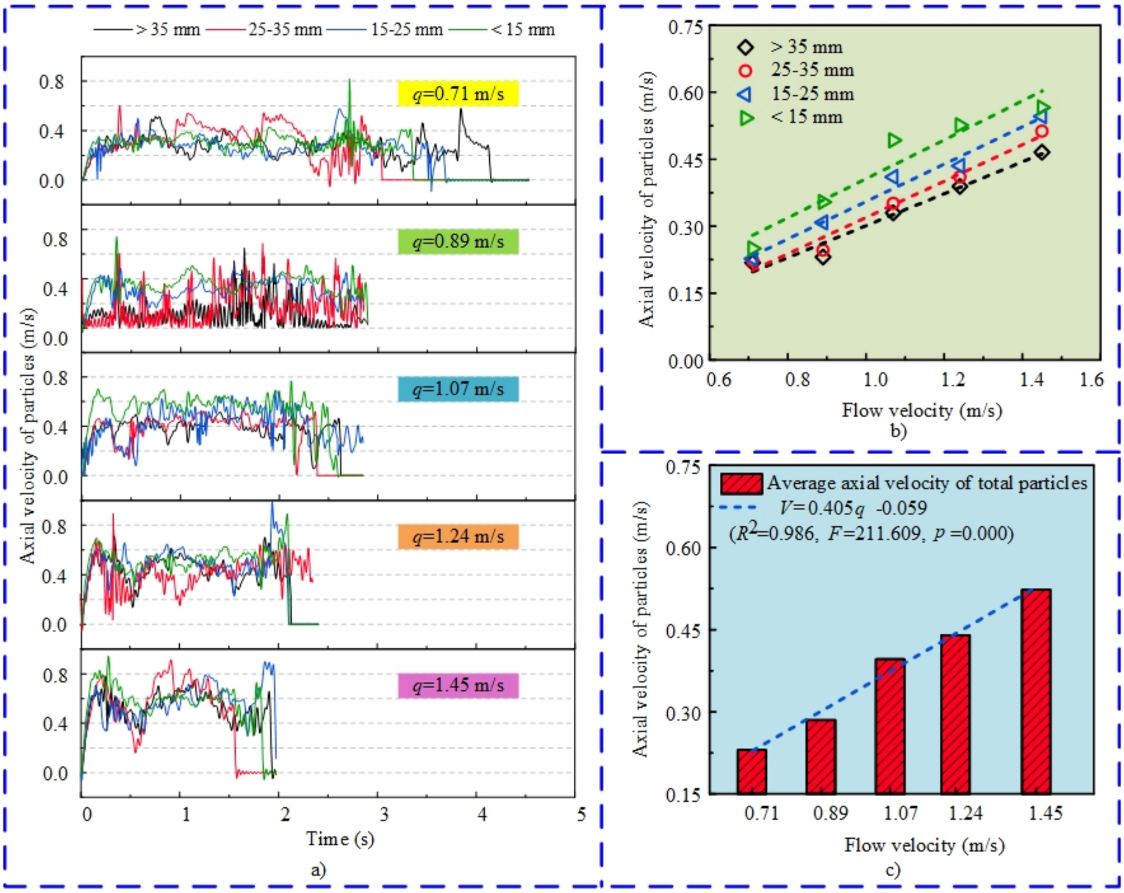

Figure 7: Axial conveying velocity of particles under different water flow velocities.

Table IV: Fitting results of different types of functions.

Regression model	Chips size	Fitting equation	R^2	F	p
Linear regression	> 35 mm	$V_z = 0.358q - 0.057$	0.968	91.458	0.002
	25–35 mm	$V_z = 0.407q - 0.088$	0.975	114.627	0.002
	15–25 mm	$V_z = 0.419q - 0.064$	0.981	156.046	0.001
	< 15 mm	$V_z = 0.437q - 0.031$	0.921	34.781	0.01
Power function regression	> 35 mm	$V_z = 1.197q^{0.298}$	0.962	684.893	0.000
	25–35 mm	$V_z = 1.286q^{0.315}$	0.973	865.201	0.000
	15–25 mm	$V_z = 1.163q^{0.353}$	0.973	976.598	0.000
	< 15 mm	$V_z = 1.035q^{0.408}$	0.890	268.463	0.000
Parabolic function regression	> 35 mm	$V_z = 0.137q^2 + 0.061q + 0.095$	0.975	39.740	0.025
	25–35 mm	$V_z = 0.190q^2 - 0.003q + 0.121$	0.985	66.463	0.015
	15–25 mm	$V_z = -0.067q^2 + 0.562q - 0.137$	0.982	55.740	0.018
	< 15 mm	$V_z = -0.521q^2 + 1.563q - 0.603$	0.987	74.800	0.013

4.3 Coupling effect of rotational speed and water flow velocity

As shown in Fig. 8, the coupling relationship between the axial velocity of particles and the rotational speed of casing and the velocity of water flow is given. When the rotational speed is low, the increase in the water flow velocity has no obvious effect on the rise in the axial migration velocity of particles. When the rotational speed further increases and exceeds 120 rpm, the increase in the speed of water flow can obviously improve the axial migration speed of particles. The rotation of the spiral casing can play a role in disturbing the drilling slag by effectively inhibiting its settlement. Thus, the flushing fluid can better play its carrying role. After fitting, the mathematical relationship between the axial migration velocity of particles and the rotational speed of casing and the velocity of water flow is as follows:

$$V_z = 0.37 - 0.036q - 0.007n - 0.046q^2 + 3.14\cdot 10^{-5}n^2 + 0.0034nq \quad (1)$$

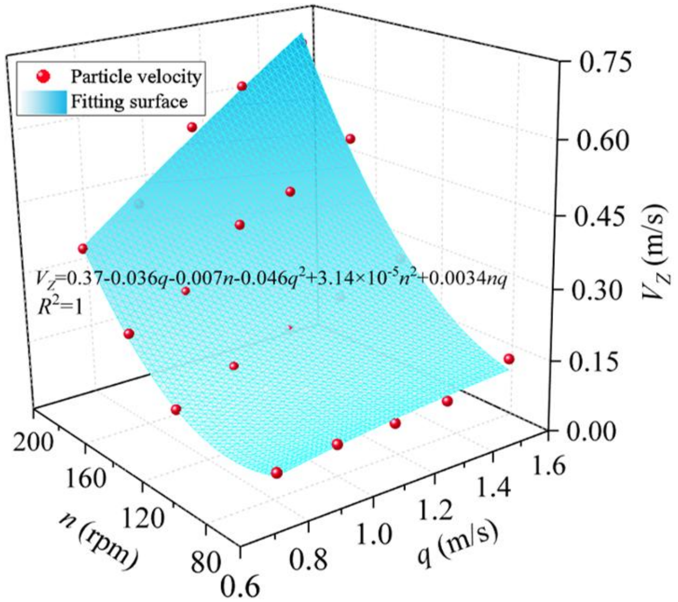

Figure 8: Axial conveying velocity of particles under different water flow velocities.

5. CONCLUSION

The coupling analysis model based on the CFD–DEM method was established in this study to determine the effect of the rotational speed of casing and the velocity of water flow in the borehole on the axial migration velocity of differently sized particles. Meanwhile, 20 sets of numerical calculations were conducted by changing the rotational speed and water flow velocity. Ultimately, the position state of particles with different particle sizes in the hole and the change curve of the axial migration velocity of particles were obtained. The specific conclusions are obtained as follows:

(1) The spiral casing has a significant improvement effect on the axial movement of particles in the auxiliary drilling, especially for the larger cutting particles. The corresponding axial flow velocity of particles is approximately 2.5 times that of the ordinary casing, which confirms the superiority of the spiral casing in improving the slag removal effect of the near-horizontal drilling.

(2) The axial conveying velocity of particles has a linear relationship with the velocity of water flow, and it has a power function relationship with the rotational speed of casing. Under the coupling effect of water flow and casing rotation, when the rotational speed is low, increasing the water flow velocity has no obvious effect on improving the axial migration velocity of particles. When the rotational speed further increases and exceeds 120 rpm, the

increase in the velocity of water flow can obviously improve the axial migration velocity of particles.

(3) In practical engineering applications, the casing should be in rotating state before opening the flushing medium. Otherwise, the flushing medium can be easily blocked due to particle deposition. The accumulated particles will lock the casing under the pressure of the flushing medium and cause an accident in the hole.

The single and coupling relationship between the axial conveying velocity of particles and the rotational speed of casing and the velocity of water flow are studied in detail in this work. The importance of the research results for engineering practice is summarized. The research provides a reference for the optimal drilling process and selection of key parameters of pipe-following drilling with spiral casing.

ACKNOWLEDGEMENT

This study was supported by the Automatic Research Fund of Key Laboratory of Xinjiang Coal Resources Green Mining (Grant No. KLXGY-Z2608), the Doctoral Start-up Fund of Xinjiang Institute of Engineering (Grant No. 2025XGYBQJ55) and the Natural Science Foundation of Xinjiang Uygur Autonomous (Grant No. 2023D01A83).

REFERENCES

[1] Yan, X.-F.; Ariaratnam, S. T.; Dong, S.; Zeng, C. (2018). Horizontal directional drilling: state-of-the-art review of theory and applications, *Tunnelling and Underground Space Technology*, Vol. 72, 162-173, doi:10.1016/j.tust.2017.10.005

[2] Qu, P.; Shen, R.-C.; Fu, L.; Wang, Z.-J. (2011). Time delay effect due to pore pressure changes and existence of cleats on borehole stability in coal seam, *International Journal of Coal Geology*, Vol. 85, No. 2, 212-218, doi:10.1016/j.coal.2010.10.013

[3] Meier, T.; Rybacki, E.; Reinicke, A.; Dresen, G. (2013). Influence of borehole diameter on the formation of borehole breakouts in black shale, *International Journal of Rock Mechanics and Mining Sciences*, Vol. 62, 74-85, doi:10.1016/j.ijrmms.2013.03.012

[4] Liu, M.; Jin, Y.; Lu, Y.-H.; Chen, M.; Hou, B.; Chen, W.-Y.; Wen, X.; Yu, X.-N. (2016). A wellbore stability model for a deviated well in a transversely isotropic formation considering poroelastic effects, *Rock Mechanics and Rock Engineering*, Vol. 49, No. 9, 3671-3686, doi:10.1007/s00603-016-1019-8

[5] Zhang, J.-C. (2013). Borehole stability analysis accounting for anisotropies in drilling to weak bedding planes, *International Journal of Rock Mechanics and Mining Sciences*, Vol. 60, 160-170, doi:10.1016/j.ijrmms.2012.12.025

[6] Liu, S.-Y.; Xu, B.-L.; Qin, L.-X.; Meng, Q.-H.; Li, H.-S. (2023). Study on long-distance fast advance drilling technology strategy and supporting equipment in coal mine roadway tunnelling, *Coal Science and Technology*, Vol. 51, No. S2, 229-239, doi:10.12438/cst.2023-0012

[7] Moreira, B. A.; de Oliveira Arouca, F.; Damasceno, J. J. R. (2017). Analysis of suspension sedimentation in fluids with rheological shear-thinning properties and thixotropic effects, *Powder Technology*, Vol. 308, 290-297, doi:10.1016/j.powtec.2016.12.034

[8] Denney, D. (2008). Pipe-rotation effect on hole cleaning for water-based drilling fluids in horizontal and deviated wells, *Journal of Petroleum Technology*, Vol. 60, No. 11, 65-68, doi:10.2118/1108-0065-JPT

[9] Li, K.; Ting, R.; Yao, Y.-F. (2023). Key technology of automatic loading and unloading system for dual-pipe directional drilling rig and its application in soft–fragmentized coal seam, *Coal Geology & Exploration*, Vol. 51, No. 4, 179-186, doi:10.12363/issn.1001-1986.22.08.0613

[10] Jin, X.; Zheng, J.; Hua, S.; Tong, X. (2025). Influencing factors of deformation and failure of porous coal under conventional loading, *Facta Universitatis, Series: Mechanical Engineering*, Vol. 23, No. 1, 161-170, doi:10.22190/FUME240304036J

[11] Ford, J. T.; Peden, J. M.; Oyeneyin, M. B.; Gao, E.; Zarrough, R. (1990). Experimental investigation of drilled cuttings transport in inclined boreholes, *Proceedings of the SPE Annual Technical Conference and Exhibition*, Paper SPE-20421-MS, 197-206, doi:10.2118/20421-ms

[12] Nguyen, D.; Rahman, S. S. (1998). A three-layer hydraulic program for effective cuttings transport and hole cleaning in highly deviated and horizontal wells, *SPE Drilling & Completion*, Vol. 13, No. 3, 182-189, doi:10.2118/51186-PA

[13] Cho, H.; Shah, S. N.; Osisanya, S. O. (2000). A three-layer modeling for cuttings transport with coiled tubing horizontal drilling, *Proceedings of the SPE Annual Technical Conference and Exhibition*, Paper SPE-63269-MS, 182-189, doi:10.2118/63269-MS

[14] Kelessidis, V. C.; Bandelis, G. E. (2004). Flow patterns and minimum suspension velocity for efficient cuttings transport in horizontal and deviated wells in coiled-tubing drilling, *SPE Drilling & Completion*, Vol. 19, No. 4, 213-227, doi:10.2118/81746-PA

[15] Hou, Z.-K.; Yuan, Y.; Chen, Y.; Jiang, E.-Y.; Wang, H.-S; Zhang, X. (2023). A review of the settling law of drill cuttings in drilling fluids, *Processes*, Vol. 11, No. 11, Paper 3165, 15 pages, doi:10.3390/pr11113165

[16] Zhang, H.; Kang, H.-P.; Xu, Y.-L. (2014). Deslagging mechanics and application of roadway floor anchor hole in coal mine, *Journal of China Coal Society*, Vol. 39, No. 3, 430-435, doi:10.13225/j.cnki.jccs.2013.0075

[17] Wang, Y.-L.; Sun, Y.-N.; Wang, Z.-F.; Song, W.-B. (2015). Mechanical characteristic of borehole clogging drilling in soft and outburst coal seam, *Journal of China Coal Society*, Vol. 40, No. S1, 119-125, doi:10.13225/j.cnki.jccs.2014.0536

[18] Pan, J.-T.; Liu, C.-Y.; Zhao, D.; Jia, N.; Liu, H.-J.; Ren, Z.-B. (2023). Downward directional drilling nitrogen foam power-law multiphase flow slag unblocking technology, *Coal Science and Technology*, Vol. 51, No. 12, 298-309, doi:10.12438/cst.2023-0862

[19] Wang, Y.-L.; Zhai, X.-X.; Sun, Y.-N. (2011). Reasonable parameters study on grooved drill pipe used in drilling outburst coal seam, *Journal of China Coal Society*, Vol. 36, No. 2, 304-307, doi:10.13225/j.cnki.jccs.2011.02.017

[20] Liu, S.-W.; Feng, Y.-L.; Dong, S.-J. (2013). Influence factors analysis and parameters optimization of deslagging in roadway floor anchoring boreholes, *Journal of China University of Mining and Technology*, Vol. 42, No. 5, 761-765, doi:10.13247/j.cnki.jcumt.2013.05.010

[21] Fu, M.-X.; Liu, S.-W.; Jia, H.-S.; Jiang, Y.-J.; Lu, Y.-H. (2022). Study on migration rules and influencing factors of the fragments ascending during boreholes drilling rock in coal mine roadway floors, *Journal of Mining and Safety Engineering*, Vol. 39, No. 3, 584-597, doi:10.13545/j.cnki.jmse.2021.0252

[22] Mao, C.-Z.; Zhang, X.-X.; Li, F.-Q.; Wu, D.-Y.; Zhang, S.-H. (2023). On cutting transport for air reverse circulation in horizontal and inclined wells, *Tunnelling and Underground Space Technology*, Vol. 136, Paper 105095, 16 pages, doi:10.1016/j.tust.2023.105095

[23] Jiang, H.-J.; Lin, L.-K.; Wen, Z.-B.; Xiao, X.-M.; Zhou, Z.-X. Xia, Y.-M. (2023). Structure effect of a suction pipe on slag-discharging performance in a shaft boring machine, *Journal of Mechanical Science and Technology*, Vol. 37, No. 9, 4647-4659, doi:10.1007/s12206-023-0820-z

[24] Lerher, T.; Grum, Z.; Motaln, M.; Zadravec, M. (2024). Wear simulation of the conveyor belt transfer chute using the DEM, *International Journal of Simulation Modelling*, Vol. 23, No. 1, 77-88, doi:10.2507/IJSIMM23-1-673

[25] Yu, Y.; Fang, P.; Zhang, B.; He, Y.-Y.; Li, G.; Xiao, D. (2023). Characteristics of cuttings migration with new cuttings removal device in horizontal well, *Geoenergy Science and Engineering*, Vol. 231, Paper 212379, 18 pages, doi:10.1016/j.geoen.2023.212379

[26] Akhshik, S.; Behzad, M.; Rajabi, M. (2015). CFD-DEM approach to investigate the effect of drill pipe rotation on cuttings transport behavior, *Journal of Petroleum Science and Engineering*, Vol. 127, 229-244, doi:10.1016/j.petrol.2015.01.017

[27] Dimaki, A.; Shilko, E.; Psakhie, S.; Popov, V. (2018). Simulation of fracture using a mesh-dependent fracture criterion in the Discrete Element Method, *Facta Universitatis, Series: Mechanical Engineering*, Vol. 16, No. 1, 41-50, doi:10.22190/FUME171229010D

[28] Cao, K.; Li, X. H.; Gao, H. D.; Zhang, L. X.; You, F. (2023). Design and analysis of a vertical screw stirring device for feeding dairy goats, *International Journal of Simulation Modelling*, Vol. 22, No. 3, 462-473, doi:10.2507/IJSIMM22-3-655